J Mater Sci (2008) 43:3189–3196
DOI 10.1007/s10853-008-2498-0

Luminescence of Cu^+ in halosulphate phosphor

**S. J. Dhoble · S. C. Gedam · I. M. Nagpure ·
S. V. Godbole · M. K. Bhide · S. V. Moharil**

Received: 25 September 2007 / Accepted: 24 January 2008 / Published online: 11 March 2008

Abstract Ultraviolet photo-excited luminescence from Cu-doped halosulphate phosphors has been investigated. The intense emission of the spectrum is assigned to electronic transitions $3d^9 4s^1 \rightarrow 3d^{10}$ in Cu^+ ions. Increase in photoluminescence (PL) peak intensity suggesting that Cu plays an important role in PL emission in the present matrix. However, limited hosts with Cu^+ as luminescence center were studied due to difficulties in incorporating it in a luminescence form. Cu-doped halosulphate phosphors were synthesized by wet chemical method. X-ray diffraction and PL characterization of phosphors has been reported in this article. The article discusses the luminescence of Cu^+ and the simple method of incorporation in various new hosts.

Introduction

Cu^+ is known to exhibit characteristic luminescence corresponding to $3d^9 4s \leftrightarrow 3d^{10}$ transitions. The incorporation of copper into several matrices provides them with interesting optical features, which strongly depend on the ionic state of the copper atoms [1–10]. In particular, the presence of Cu^+ ions in different matrices activates a luminescent emission in the ultraviolet (UV) and visible (VIS) range of the spectrum [1–6], that arises potential applications of these materials for the realization of tunable lasers [3, 7], and other optical devices [8–10]. Special interest has been paid to the incorporation of copper into matrices such as sulphates, because they are technologically simple to obtain and conform at low cost even for large size. Among the different techniques employed to prepare these materials, wet chemical process appears as a promising route. It is a low-temperature process and the amount of metal that can be introduced preserving the ionic state is large when compared with other traditional methods of preparation.

Schemes for using this emission for lasing have been proposed [11, 12]. Proposals have also been made to use photo-stimulated luminescence of Cu^+ for X-ray imaging [13–15]. Cu^+ emission has also been used in thermo luminescence dosimetry phosphors such as LiF:Mg, Cu, P [16], $Li_2B_4O_7$:Cu [17, 18] Cu^+ emission can also be used as blue component of full color electro luminescent display devices [19, 20]. However, more common valency of copper is 2^+, and the methods for incorporating monovalent Cu have not been systematically worked out, e.g., in several works results on Cu^+ emission in alkali halides have been mentioned [21–30], but the procedure adopted for incorporating Cu in monovalent form has not been given. Several authors on the other hand, mention that incorporation of Cu^+ can be difficult [31]. The presence of OH^- ions hampers such incorporation, and phosphor preparation in dry argon/halogen atmosphere has been advocated. Notwithstanding the data on Cu^+ presented in earlier works [32] doping of Cu^+ has been achieved in a limited number of solids, and incorporation of monovalent copper in lattices such as fluorides is still considered to be difficult [33–35].

S. J. Dhoble · I. M. Nagpure
Kamla Nehru College, Sakkardara Square, Nagpur 440009, India

S. C. Gedam (✉)
K.Z.S. Science College, Kalmeshwar, Nagpur 441501, India
e-mail: gedam_sc@rediffmail.com

S. V. Godbole · M. K. Bhide
Spectroscopy Section, Radiochemistry Division, BARC,
Mumbai 400085, India

S. V. Moharil
Department of Physics, R.T.M. Nagpur University,
Nagpur 440033, India

Cuprous halide nanocrystal is one of the most widely used materials for study of quantum-size confinement of exciton translational motion. The exciton absorption spectra of bulk crystals of the cuprous halides CuCl, CuBr, and CuI consist of two intense narrow bands, which are called $Z_{1.2}$ and Z_3 bands. The energy of the Z_3 exciton band is lower than that of the $Z_{1.2}$ exciton in CuCl, while the energy of the $Z_{1.2}$ exciton is lower than that of the Z_3 exciton in CuBr and CuI, because the contribution of the copper ion with negative spin–orbit interaction to the valence band is larger in CuCl than in CuBr and CuI. We have successfully used the technique in doping Cu^+ in solids, which could be interesting for several reasons.

Other than sulphates and mixed sulphates, some investigations are going in progress on halosulphate-based materials. Klement [36] synthesized the halosulphate material $Na_6Ca_4(SO_4)_6F_2$ and characterized this compound by X-ray powder diffraction. Also, the compounds $Na_6Pb_4(SO_4)_6Cl_2$ [37, 38], $Na_6Cd_4(SO_4)_6Cl_2$ [39], and $Na_{6.45}Ca_{3.55}(SO_4)_6(F_xCl_{1-x})_{1.55}$ [40]. Recently, we have reported $KZnSO_4Cl$ and $KMgSO_4Cl$ [41, 42] halosulphate phosphors as the new luminescent materials and characterized photoluminescence (PL) by doping Ce, Dy, and Mn. Data on PL of Cu^+ in these hosts are presented in this article.

Experimental

The samples $KZnSO_4Cl$, $KMgSO_4Cl$, Na_3SO_4F, $NaMgSO_4F$ (pure), and Cu doped were prepared by a wet chemical method. In case of $ZnSO_4$ and KCl of analar grade were taken in a stoichimetric ratio and dissolved separately in double distilled deionized water, resulting in a solution of $KZnSO_4Cl$ (Eq. 1). In the present experiment, we used $CuCl_2$ added to the solution to obtain $KZnSO_4Cl$:Cu. Confirming that no undissolved constituents were left behind, and all the salts had completely dissolved in water and thus reacted.

$$ZnSO_4 + KCl \rightarrow KZnSO_4Cl \tag{1}$$

The compounds $KZnSO_4Cl$ (pure); $KZnSO_4Cl$:Cu in its powder form was obtained by evaporating at 80 °C for 8 h. The dried samples were then slowly cooled at room temperature. The resultant polycrystalline mass was crushed to fine particle in a crucible. The powder was used in further study. Similar method was adopted for $KMgSO_4Cl$, Na_3SO_4F and $NaMgSO_4F$ pure and Cu-doped samples shown by the following equations.

$$MgSO_4 + KCl \rightarrow KMgSO_4Cl \tag{2}$$

$$Na_2SO_4 + NaF \rightarrow Na_3SO_4F \tag{3}$$

$$MgSO_4 + NaF \rightarrow Na_3SO_4F \tag{4}$$

Formation of the compound was confirmed by taking the X-ray diffraction (XRD) pattern that matched with the standard data available (as shown in Table 1). The PL emission spectra of the samples were recorded using Fluorescence spectrometer (Hitachi F-4000) fitted with a sensitive photomultiplier. This spectrofluorometer provides corrected emission and excitation spectra in the 250–720

Table 1 XRD data of studied samples

Samples	Angle (2θ)	Relative intensity (%)	Samples	Angle (2θ)	Relative intensity (%)	Samples	Angle (2θ)	Relative intensity (%)
$KMgSO_4Cl$	12.73	25		18.33	15		29.8	56.21
	24.03	65.75		22.81	45		32.87	83.65
	25.80	20		23.36	43		34.93	79.89
	26.12	50.7		24.80	65		36.84	22.19
	28.69	21		25.10	51		39.37	22.09
	28.96	21		29.20	100		42.04	39.24
	30.23	100		30	60		52.44	45.95
	30.84	47		31.23	32.66	$NaMgSO_4F$	12.6	19
	31.23	47		36	25		22.01	70
	31.61	49		40	19		27.15	75
	42.88	52		41	19		30.37	100
	49.10	19.2		48	15		32.05	53
	64	34						Na_3SO_4F
	20.67	33.84	42.83	80				
72.75	17.5		23.38	66.66	53.44		22	
$KZnSO_4Cl$	12.19		25	25.54	100	62.2	48	

and 230–700 range, respectively. The same amount of sample was used in each case. Emission and excitation spectra were recorded using a spectral slit width of 1.5 nm.

Results and discussion

Cu^+ emission in $KMgSO_4Cl$

In most sulphates Cu is incorporated in divalent form when these phosphors were prepared by the conventional techniques of mixing through solutions or by melting appropriate sulphates, no Cu^+ emission was observed. The phosphors prepared by wet chemical technique, on the other hand, exhibited bright violet/blue emission. For $KMgSO_4Cl$, the emission maxima are around 420 nm. It has earlier been observed that depending on the method of incorporation, Cu^+ PL characteristics in same hosts can change. This is especially true for hosts in which the straightforward methods do not lead to the incorporation of Cu^+. The emission maximum is located at 420 nm, while the excitation maximum is at 257 nm. Cu^+ emission was observed in the alkali sulphates as well [43].

Figure 1 shows XRD pattern of $KMgSO_4Cl$ prepared material match with standard data of $KMgSO_4Cl$. The PL excitation spectra of $KMgSO_4Cl:Cu^+$ phosphor (Fig. 2) shows broadband is observed at 257 nm with a prominent shoulder around 220 nm ($\lambda_{em} = 420$ nm). Figure 3 shows the PL emission spectra of Cu^+ ions in $KMgSO_4Cl$ phosphors with different concentration under excitation 257 nm wavelengths of light. The peaks are observed at 420, 413, 420, and 463 nm for 0.5, 0.3, 0.2, and 0.1 mole % concentrations, respectively, which are assigned to the $3d^94s \leftrightarrow 3d^{10}$ transition of Cu^+ ions. With increasing concentration of Cu^+ ions the peak intensity increases and maximum intensity is observed for 0.5 mole % of Cu^+ ion (shown in Figs. 3 and 4). This indicates that the $KMgSO_4Cl$ lattice more suitable for higher concentrations of Cu^+ ions. It has earlier been observed that depending on the method of incorporation, Cu^+ PL characteristics in same hosts can change. This is especially true for hosts in which the straightforward methods do not lead to the incorporation of Cu^+. In [44], no explanation has been offered as to how monovalent copper was incorporated.

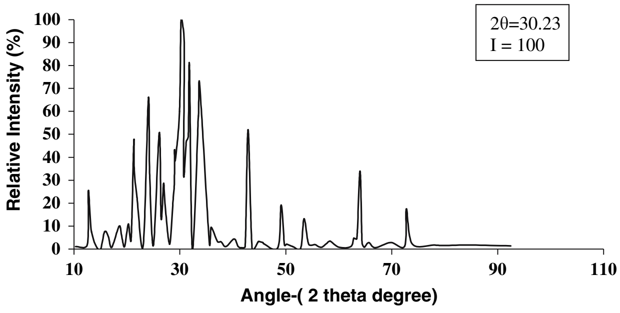

Fig. 1 X-Ray diffraction pattern (XRD) of $KMgSO_4Cl$

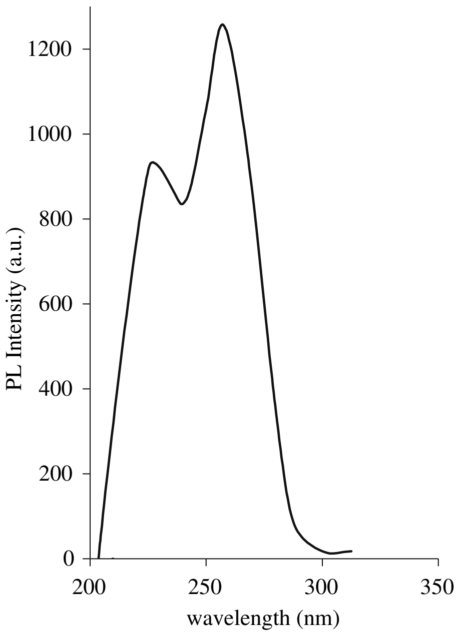

Fig. 2 PL excitation spectra of $KMgSO_4Cl:Cu_{0.5\ mole\%}$

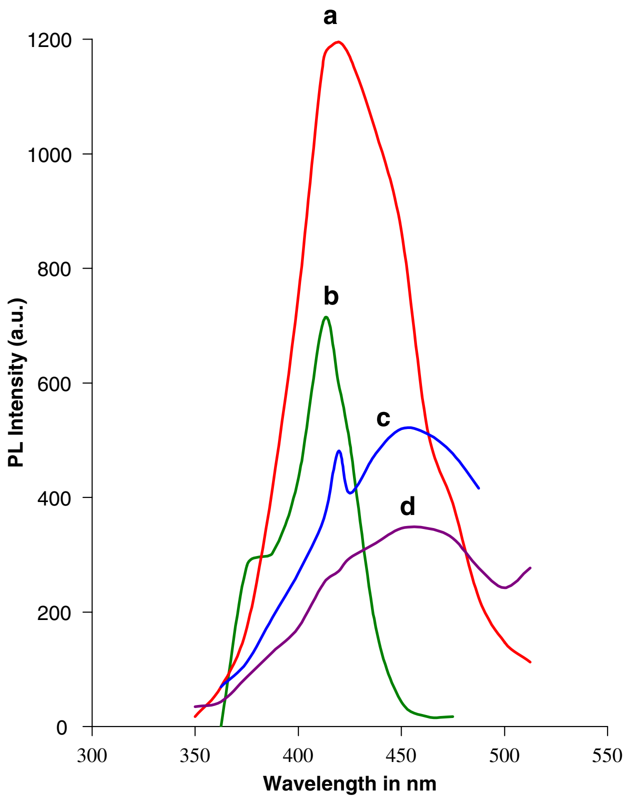

Fig. 3 PL emission spectra of $KMgSO_4Cl:Cu$ (**a**) 0.5 mole %, (**b**) 0.3 mole %, (**c**) 0.2 mole %, (**d**) 0.1 mole % (for $\lambda_{exc} = 257$ nm)

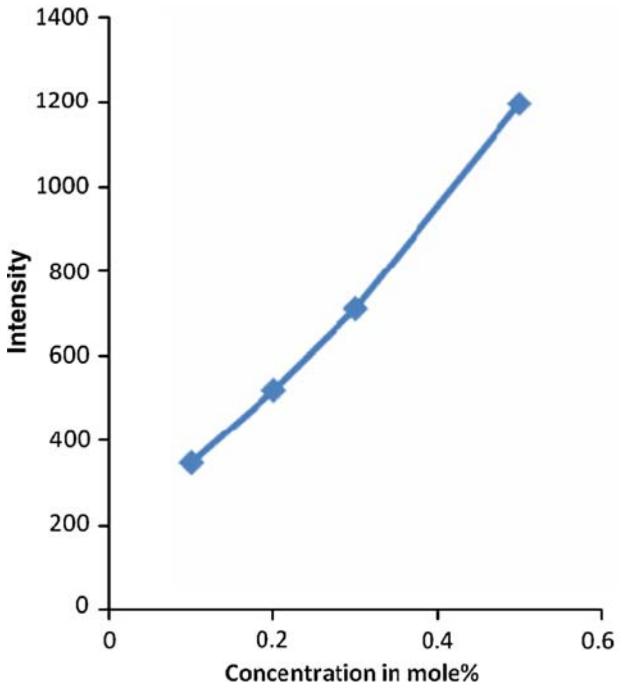

Fig. 4 Increased intensity with increased

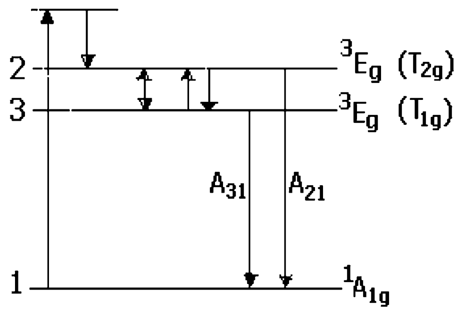

Fig. 5 Energy level diagram showing the states concentration involved in the luminescence process and the transition probabilities

Cu-doped luminescence was excited with UV light [45]. The emission spectrum spreads over the VIS range with the maximum at about 463 nm as it is shown in Fig. 3. Several emission bands from both crystalline and glassy copper-doped materials have been reported in the VIS range of the spectrum, all of them associated to electronic transitions $d^{10} \leftrightarrow d^9s^1$ in Cu^+ ions [45–49]. The site symmetry of the Cu^+ ions and the covalence degree of copper–oxygen bond determine mainly the shape of the spectrum. Emission bands peaking at the green region of the spectrum are originated by Cu^+ ions in tetragonal distorted sites [46, 47].

Figure 5 shows energy level diagram indicating the states involved in the luminescence process and the transition probabilities for Cu^+ ions. According to that model, the system is first excited from the ground state ($3d^{10}$ configuration) to the singlet state of the $3d^94\,s^1$ configuration and then, the electrons pass to the triplet state, mainly to level 2 because of symmetry reasons [46–49]. The last transition is so much faster than any other step of the luminescent process, that it may be considered instantaneous; it follows that the singlet state does not affect the luminescent process. Nonradiative transitions may occur between the two energy levels of the triplet state, named 2 and 3 with probabilities p_{23} (from level 2 to level 3), and p_{32} (from level 3 to level 2). From levels 2 and 3, radiative transitions to the ground state (level 1) occur with probabilities A_{21} and A_{31}, respectively. The intensity of Cu^+ emission at 463 nm is less, as compared to that of

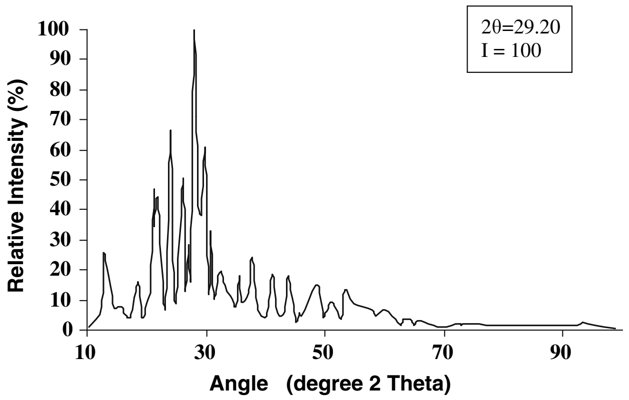

Fig. 6 XRD pattern of $KZnSO_4Cl$

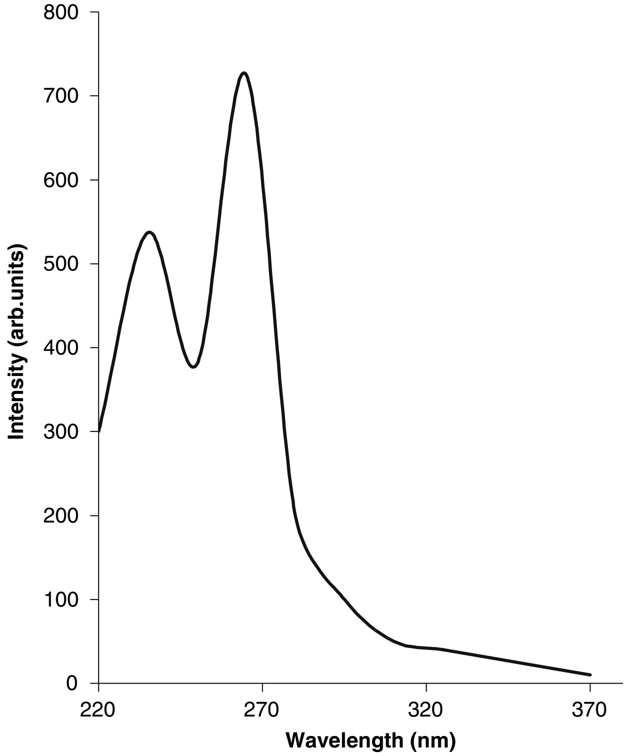

Fig. 7 PL excitation spectra of $KZnSO_4Cl:Cu$

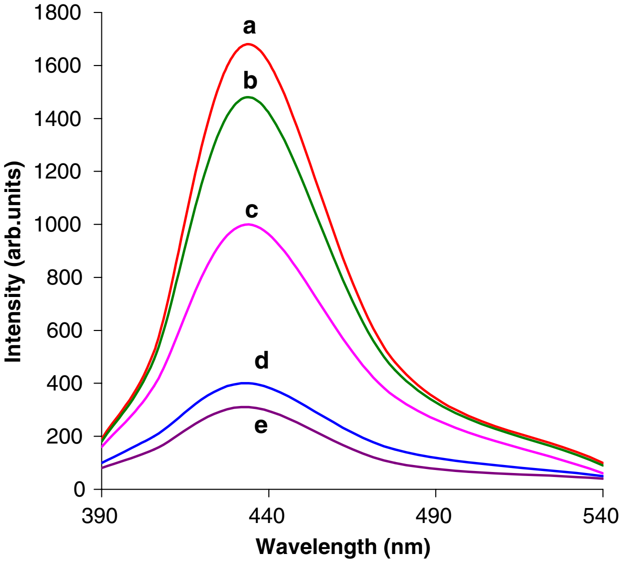

Fig. 8 PL emission spectra of $KZnSO_4Cl$:Cu 0.5 mole % (for $\lambda_{emi} = 434$ nm) (**a**) 0.5 mole %, (**b**) 0.3 mole %, (**c**) 0.2 mole %, (**d**) 0.1 mole %, and (**e**) 0.05 mole % (for $\lambda_{exc} = 259$ nm)

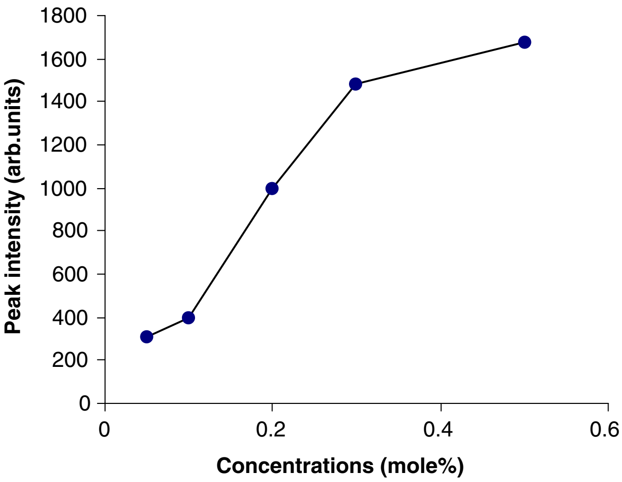

Fig. 9 Increased intensity with increased concentration

420 nm peak. The increase of PL emission intensity observed may be due to the decrease of cross relaxation between Cu^+ ions (in this process, excited ion transfers only part of energy to another ion) in case of higher concentration of Cu^+.

Cu^+ emission in $KZnSO_4Cl$

By adopting the same method $KZnSO_4Cl$:Cu-doped halo-sulphate has been prepared for 0.5, 0.3, 0.2, 0.1, and 0.05 mole % of concentrations. $KZnSO_4Cl$ (pure) compound was confirmed by taking the XRD pattern (Fig. 6), confirming that no undissolved constituents were left behind, and all the salts had completely dissolved in water and thus reacted. Incorporation of Cu in chloride material is difficult, Nanto et al. [50] have reported BaFCl:Cu phosphors, but the valency and PL of Cu were not studied. Using wet chemical method, we could dope Cu in monovalent form. Figures 7 and 8 show the excitation and emission spectra of Cu^+. The excitation maximum is at 259 nm while the emission is maximum around 440 nm. There is also a weaker emission at 440 nm for 0.05 mole % of concentration. This indicates that the $KZnSO_4Cl$ lattice more suitable for higher concentrations of Cu^+ ions (Fig. 9). The results are summarized in Table 2.

Table 2 Summary of PL data

Phosphors	Emission wavelength (nm)	PL intensity
$KMgSO_4Cl$:Cu 0.5%	420	1195
$KMgSO_4Cl$:Cu 0.3%	413	710
$KMgSO_4Cl$:Cu 0.2%	420, 450	480, 520
$KMgSO_4Cl$:Cu 0.1%	463	347
$KZnSO_4Cl$:Cu 0.5%	434	1680
$KZnSO_4Cl$:Cu 0.3%	434	1480
$KZnSO_4Cl$:Cu 0.2%	434	995
$KZnSO_4Cl$:Cu 0.1%	434	400
$KZnSO_4Cl$:Cu 0.05%	434	310
Na_3SO_4F:Cu 1%	440	625
Na_3SO_4F:Cu 0.5%	440	400
$NaMgSO_4F$:Cu 0.5%	420	825
$NaMgSO_4F$:Cu 0.3%	420	775
$NaMgSO_4F$:Cu 0.2%	420	725
$NaMgSO_4F$:Cu 0.1%	420	300

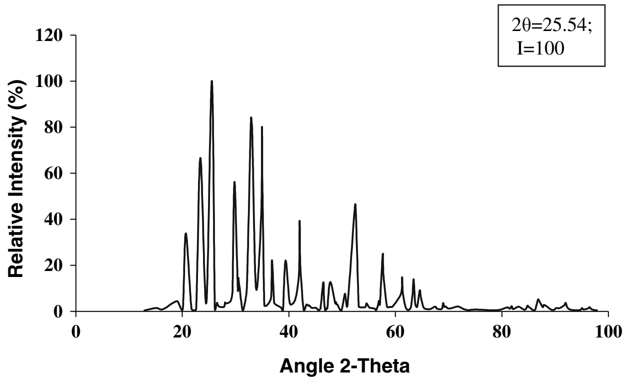

Fig. 10 XRD pattern of Na_3SO_4F

Cu^+ emission in Na_3SO_4F

In most sulphates Cu is incorporated in divalent form when these phosphors were prepared by the conventional techniques of mixing through solutions or by melting appropriate sulphates, no Cu^+ emission was observed. Cu^+

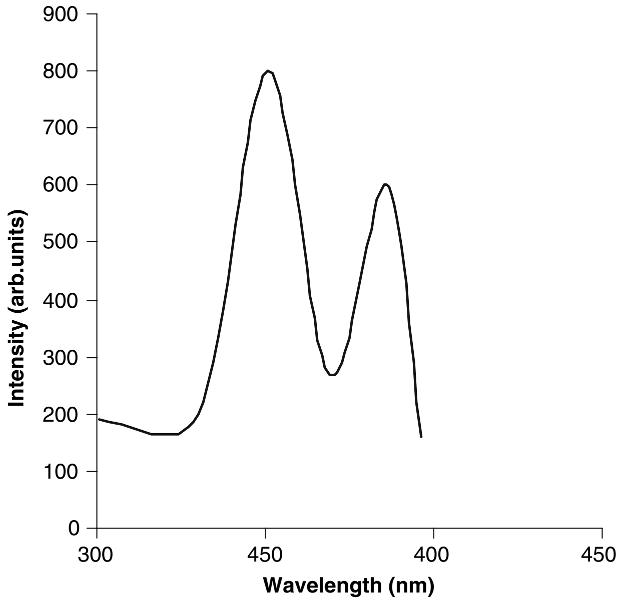

Fig. 11 PL excitation spectra of Na_3SO_4F:Cu

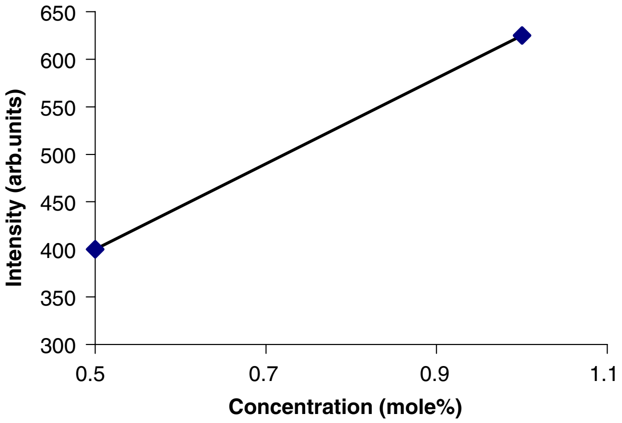

Fig. 12 Increased intensity with increased concentration

emission was observed in the mixed alkali sulphate as well. The phosphors prepared by this technique, on the other hand, exhibited bright violet/blue emission. Figure 10 shows XRD pattern of Na_3SO_4F (pure). It has earlier been observed that depending on the method of incorporation, Cu^+ PL characteristics in same hosts can change. Figure 11 shows the excitation spectra of Na_3SO_4F:Cu having two maxima well separated to each other. The excitation maximum is at 350 nm while the emission maximum is located at 440 nm. Though this material is also suitable for higher concentration (Fig. 12), it is found that, the PL emission was not observed for <0.5 mole % concentration (Na_3SO_4F:Cu phosphor not suitable for 0.3, 0.2, 0.1, and 0.05 mole % concentrations), therefore 1 and 0.5 mole % of concentrations was considered. Figure 13 shows PL emission spectra of Na_3SO_4F:Cu.

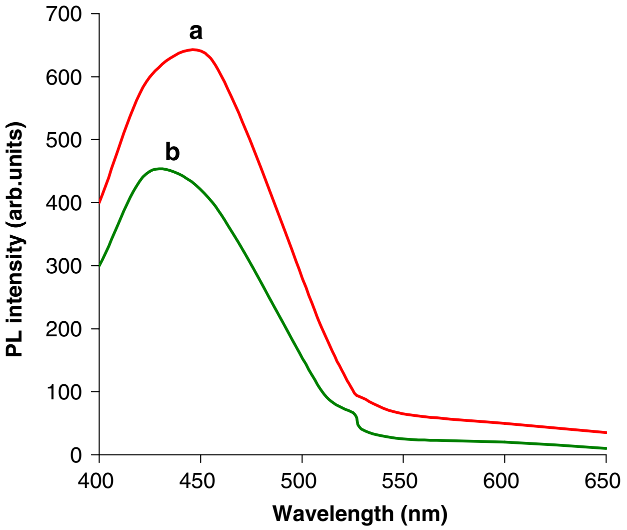

Fig. 13 PL emission spectra of Na_3SO_4F:Cu 0.5 mole % (for $\lambda_{emi} = 440$ nm) (**a**) 1 mole % and (**b**) 0.5 mole % (for $\lambda_{exc} = 350$ nm)

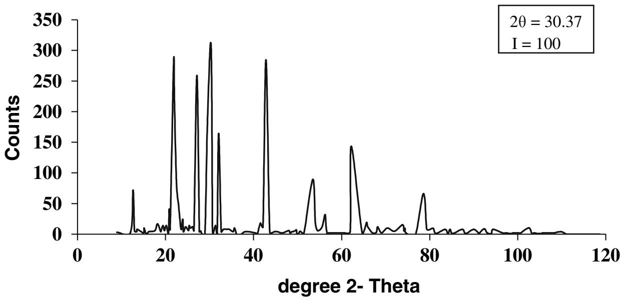

Fig. 14 XRD pattern of $NaMgSO_4F$

Cu^+ emission in $NaMgSO_4F$

Cu^+ emission was observed in $NaMgSO_4F$ prepared by wet chemical method. Figure 14 shows XRD pattern of $NaMgSO_4F$. The excitation maximum is conveniently achieved by 385 nm (Fig. 15) where as the emission is situated in the UV region peaking at 420 nm. Figure 16 shows PL spectra for 0.5, 0.3, 0.2, and 0.1 mole % concentrations (for $\lambda_{exc} = 385$ nm) peaking at 420 nm of wavelength. The PL data are summarized in Table 2. As the various Cu^+ phosphors prepared have differing crystal structures. Figure 17 shows the increase in intensity as the concentration of dopants are increased.

Conclusions

Cu^+ emission could be observed in halosulphate based various hosts notwithstanding earlier works. From the characterization, it is clear that for 0.5 mole % concentration of $KMgSO_4Cl$:Cu, $KZnSO_4Cl$:Cu, and $NaMgSO_4F$:Cu

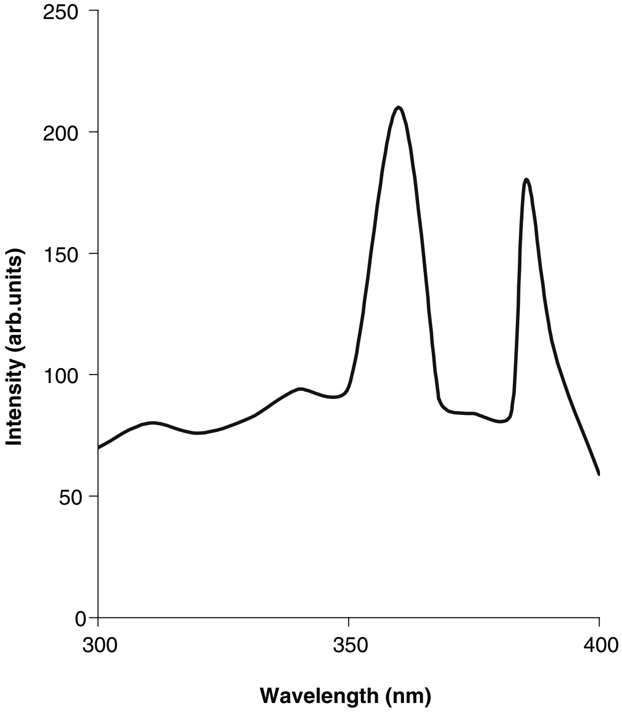

Fig. 15 PL excitation spectra of $NaMgSO_4F$:Cu

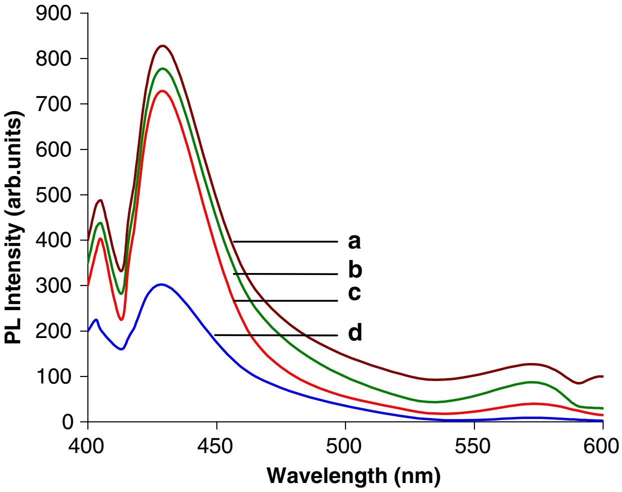

Fig. 16 PL emission spectra of $NaMgSO_4F$:Cu 0.5 mole % (for $\lambda_{\mathrm{emi}} = 420$ nm) (**a**) 0.5 mole %, (**b**) 0.3 mole % (**c**) 0.2 mole %, and (**d**) 0.1 mole % (for $\lambda_{\mathrm{exc}} = 385$ nm)

compounds; highest intensity is observed (PL emission) except Na_3SO_4F:Cu. Cu^+ emission due to $3d^94s \leftrightarrow 3d^{10}$ transition of Cu^+ ion in the hosts. All the results we are reporting first time in present halosulphate phosphors. This material can be applied to nuclear physics, X-ray and neutron diffraction, nondestructive evaluation, treaty verification and safeguards, environmental monitoring, and geological exploration. Moreover, full understanding of the nature of the competing processes and the dynamics of hole trapping by Cu^+ is still one of the challenging subjects in scintillation mechanism research.

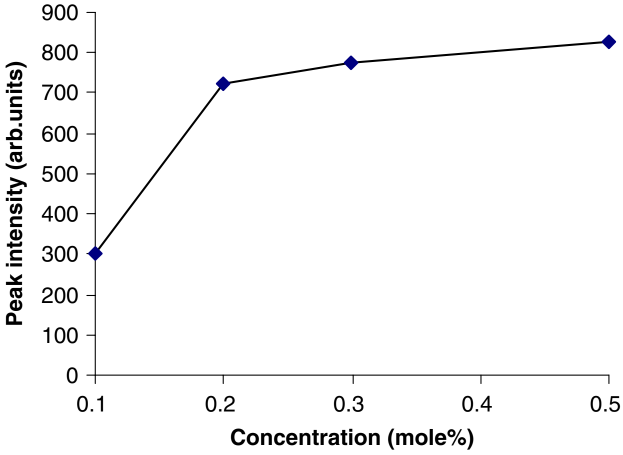

Fig. 17 Increased intensity with increased concentration

Acknowledgements Authors are indebted to Director, NEERI, Nagpur for providing facilities. SJD is thankful to BRNS, Department of Atomic Energy, Government of India, for the financial support.

References

1. Pedrini C (1978) Phys Stat Sol B 87:273
2. Pedrini C, Jaquier B (1980) J Phys C 13:4791
3. Debnath R, Das SK (1989) Chem Phys Lett 155:52
4. Debnath R, Kumar S (1990) J Non-Cryst Solids 123:271
5. Villegas MA, García MA, Llopis J, Fernández-Navarro JM (1998) J Sol-Gel Sci Technol 11:251
6. Berg JM, Chien RL, McClure DS (1987) J Chem Phys 87:7
7. Barre JD, Dumm B, Staffsudd OM, Nelsson P (1987) J Lumin 34:303
8. D'Acapito F, Colonna S, Mobilio S, Gonella F, Cattarruza E, Mazzoldi P (1997) Appl Phys Lett 71:2611
9. Gonella F, Caccavale F, Bogomolova LD, D'Acapito F, Quaranta A (1998) J Appl Phys 83:1200
10. Gonella F, Knystautas EJ, Mattei G, Mazzoldi P, Meneghini C, Cattaruzza E, Garrido F, Osborne DH (1997) Nuc Inst Meth Phys Res B 127:562
11. Boulon G (1987) In: Di Bartolo B (ed) Spectroscopy of solid state laser type materials, Plenum Press, New York, pp 223–266
12. Le Flem G (1992) J Alloys Compd 188:36
13. Nanto H, Usuda T, Sokooshi H, Nakamura S, Inabe K, Takeuchi N (1993) Sens Actuators B 10:197
14. Bandopadhaya PK, Russel GW, Chakraborti K (1999) Radiat Meas 30:51
15. Masumoto Y, Ogaswara S (1999) Jpn J Appl Phys Lett 38:L623
16. Gundurao TK, Sarwade JR, Moharil SV (1996) Radiat Eff Defect Solids 138:177
17. Shahare DI, Deshmukh BT, Moharil SV, Dhopte SM, Muthal PL, Kondawar VK (1994) Phys Stat Sol (a) 141:329
18. Martini M, Furetta C, Sanipoli C, Scacco A, Sommaiah TK (1995) Radiat Eff Defect Solids 135:133
19. Park W, Jones TC, Summers CJ (1999) Appl Phys Lett 74:1785
20. Ohmi K, Yamabe K, Fukuda H, Fujiwara T, Tanaka S, Kobayashi H (1998) Appl Phys Lett 73:1889
21. Fussgaenger K (1969) Phys Stat Sol 34:157

22. Fussgaenger K (1969) Phys Stat Sol 36:645
23. Holland U, Lüty F (1979) Phys Rev B 19:4298
24. Baldini G, Jean A, Spinolo G (1968) Phys Stat Sol 25:558
25. Krätzig E, Timusk T, Martienssen W (1965) Phys Stat Sol 10:709
26. Moine B, Pedrini C (1984) Phys Rev B 30:992
27. Boutinauad P, Parent C, Le Flem G, Pedrini C, Moine B (1992) J Phys Condens Matter 4:3031
28. Oggioni R, Scaramelli P (1965) Phys Stat Sol (b) 9:411
29. Pedrini C (1978) Phys Stat Sol (b) 87:273
30. Bosi L, Gallo D, Zelada M (1996) Nuovo Cimento D 18:605
31. Bohun A, Dolejsi J (1972) Czech J Phys B 22:737
32. Bertolaccini M, Gagiardelli P, Padovini G, Spinolo G (1976) J Lumin 14:281
33. Mcclure DS, Weaver SC (1991) J Phys Chem Solids 52:81
34. Ramsheshan SK, Payne SA (1990) Physica B 167:56
35. Goldberg AB, McClure DS, Pedrini C (1982) Chem Phys Lett 87:508
36. Klement R (1939) Naturwissenschaften 27:568
37. Schneider W, Jahrb N, Miner F (1967) Monatschefte 284
38. Schneider W, Jahrb N, Miner F (1969) Monatschefte 58
39. Kim HJ, Jeong DY, Zalar B, Blinc R, Choh SH (2000) Phys Rev B 61:9307
40. Piotrowski A, Kahlenberg V, Fischer RX (2002) J Solid-State Chem 163:398
41. Gedam SC, Dhoble SJ, Moharil SV (2006) J Lumin 121(2):450
42. Gedam SC, Dhoble SJ, Moharil SV (2007) J Lumin 124(1):120
43. Patil RR, Moharil SV (2001) Phys Stat Sol (a) 187(2):557
44. Kishan Kumar VS, Acharyulu BSVSR, Sastry SBS (1993) Phys Stat Sol (b) 175:287
45. Pedrini C (1978) Phys Stat Sol B 87:273
46. Pedrini C, Jaquier B (1980) J Phys C 13:4791
47. Debnath R, Das SK (1989) Chem Phys Lett 155:52
48. Debnath R, Kumar S (1990) J Non-Cryst Solid 123:271
49. Villegas MA, Garcia MA, Llopis J, Fernandez-Navarro JM (1998) J Sol-Gel Sci Technol 11:251
50. Nanto H, Usuda T, Sokooshi H, Nakamura S, Inabe K, Takeuchi N (1993) Sens Actuators B 10:197